SORLA regulates calpain-dependent degradation of synapsin

Hartl, D. and Nebrich, G. and Klein, O. and Stephanowitz, H. and Krause, E. and Rohe, M.

Alzheimer's & Dementia
2016 SEP; 12(9): 952-963
2016 MAR 25 (first published online)
doi: 10.1016/j.jalz.2016.02.008

Publisher: Elsevier

SORLA regulates calpain-dependent degradation of synapsin

Daniela Hartl[1,2,§], Grit Nebrich[1], Oliver Klein[1], Heike Stephanowitz[3], Eberhard Krause[3], and Michael Rohe[4§]

[1]Institute for Medical Genetics and Human Genetics, Charité - University Medicine 13353 Berlin, Germany [2]Department of Psychiatry and Psychotherapy, Saarland University Hospital, Saarland University, 66424 Homburg, Germany, [3] Leibniz Institute for Molecular Pharmacology, and [4] Max-Delbrueck-Center for Molecular Medicine, 13125 Berlin, Germany.

[§]Correspondence to: Daniela Hartl

Department of Psychiatry and Psychotherapy, Saarland University Hospital

Kirrberger Str. 1, D-66421 Homburg, Germany

Phone: +49 6841 1626355

Email: daniela.hartl@uniklinikum-saarland.de

Michael Rohe

AbbVie Deutschland GmbH & Co. KG;

Knollstraße 50, D-67061, Ludwigshafen, Germany

Email: michael.rohe@abbvie.com

ABSTRACT

INTRODUCTION: SORLA is an intracellular sorting receptor in neurons and a major risk factor for Alzheimer disease.

METHODS: Here, we performed global proteome analyses in the brain of SORLA-deficient mice followed by biochemical and histopathological studies to identify novel neuronal pathways affected by receptor dysfunction.

RESULTS: We demonstrate that lack of SORLA results in accumulation of phosphorylated synapsins in cortex and hippocampus. We propose an underlying molecular mechanism by demonstrating that SORLA interacts with phosphorylated synapsins through 14-3-3 adaptor proteins to deliver synapsins to calpain-mediated proteolytic degradation.

DISCUSSION: Our results suggest a novel function for SORLA in control of synapsin degradation, potentially impacting on synaptic vesicle endo-/exocytosis.

1. BACKGROUND

Sorting-related receptor with A-type repeats (SORLA, also known as LR11) is a member of the VPS10P domain receptor gene family, a unique class of type-1 membrane proteins expressed in the mammalian nervous system [1,2]. Initially, these orphan receptors were recognized by their structural similarity to the vacuolar protein sorting 10 protein (VPS10P), a trafficking receptor in yeast that sorts target proteins between Golgi and endosomal compartments [3]. However, recently, VPS10P domain receptors emerged as central regulators of neuronal viability and function implicated in many diseases of the nervous system including frontotemporal lobar degeneration [4], Alzheimer disease (AD) [5,6], and bipolar disorders [7].

SORLA is best known for its activity as sorting receptor for the amyloid precursor protein (APP), the main etiologic agent in AD. According to current concepts, SORLA inhibits trafficking of APP into cellular compartments where secretases reside, thereby reducing the extent of proteolytic breakdown of this precursor into neurotoxic amyloid-β peptides. Based on cumulative evidence from studies in cultured cells [5,8,9] in animal models [2,10] and in humans [6], SORLA is now considered a major risk factor for the sporadic form of AD (reviewed in [11]).

Although its contribution to amyloidogenic processes is well appreciated, there are reasons to believe that the function of SORLA in the nervous system may not be restricted to the control of APP transport and processing. Thus, transcription of *Sorl1* (the gene encoding SORLA) in neurons is strongly induced by brain-derived neurotrophic factor (BDNF), implicating this receptor in neurotrophin-dependent pathways [12].

To elucidate hitherto unknown functions for SORLA in the nervous system, we used an unbiased proteomics approach to compare the brain proteome of SORLA-deficient and control mice. Our studies uncovered up-regulation of several phosphorylated (active) forms of synapsin 1 and 2 as a consequence of receptor dysfunction. Using biochemical, and

histopathological studies, we show that SORLA physically interacts with phospho-synapsins and promotes the turnover of these synaptic vesicle (SV) -associated proteins by the protease calpain. Our results suggest a novel function for SORLA as modulator of neuronal endo-/exocytosis.

2. RESULTS

2.1 Proteins related to synaptic endo-/exocytosis are altered in the brain of SORLA-deficient mice.

We used a two-dimensional polyacrylamid gel electrophoresis (2D-PAGE) approach to compare the cortical proteome of one month old SORLA-deficient and control mice. 2D-PAGE analysis documented 94 significantly altered protein spots in *Sorl1*$^{-/-}$ compared to *Sorl1*$^{+/+}$ cortices (Student´s *t*-test, $p<0.05$; n=6 biological replicates). Subsequent analysis by mass spectrometry revealed the identity of 53 of these spots (Suppl. table 1A). A representative gel image of mouse cortex is shown in Suppl. Fig. 1. Enrichment analysis of the dataset compared to the whole mouse genome dataset or to a dataset of murine brain proteins present in 2D-PAGE [13] identified the gene ontology term “synaptic transmission” - among other functions- as being significantly enriched in this set of altered proteins ($p=6.57*10^{-6}$ and $p=2.20*10^{-3}$, respectively). The full result of the enrichment analysis is shown in Suppl. Fig. 2.

We also performed 2D-PAGE analysis on hippocampal extracts. As in cortex, we found predominant alterations in proteins related to synaptic endo-/exocytosis. Altogether, 90 protein spots were significantly altered in *Sorl1*$^{-/-}$ compared to *Sorl1*$^{+/+}$ hippocampi (Student´s t-test, $p<0.05$; n=6 biological replicates). Of these, 58 spots were identified by mass spectrometry (Suppl. table 1B). Analysis revealed enrichment of the gene ontology term “transmission of nerve impulse” when compared to the whole mouse genome dataset or to the dataset of murine brain proteins in 2D-PAGE [13] ($p=6.00*10^{-4}$ and $p=7.30*10^{-3}$, respectively, Suppl. Fig. 2).

When comparing our two datasets, we identified two protein families that were changed in expression in both, hippocampus and cortex, of *Sorl1*$^{-/-}$ mice, indicating a more

direct functional connection to SORLA. These two protein families were synapsins and 14-3-3 adaptor proteins, both of which are related to synaptic endo-/exocytosis.

2.2 Phosphorylated synapsins accumulate in the brain of SORLA-deficient mice.

Several protein spots representing modified forms of synapsins 1 and 2 were significantly increased in abundance in cortex and hippocampus of *Sorl1*$^{-/-}$ animals (Suppl. table1; Fig. 1A). Quantification of the respective spot volumes documented an approximate ratio of 1.5 to 1.8 in cortex of receptor-deficient compared to control animals (Fig. 1B; $p<0.05$). Similar increases were seen for synapsin 1 (ratio 1.7; $p=0.01$) and synapsin 2 (ratio 1.3; $p=0.02$) in hippocampus (Suppl. table 1B).

Synapsins are phospho-proteins with eight phosphorylation sites functionally characterized so far. Typically, phosphorylation induces mobilization of SV that are sequestered by synapsins otherwise (reviewed in [14]). Because accumulation of synapsins was seen for multiple iso-spots in our 2-D gels, indicative of alternative post-translational modification, we tested the phosphorylation status of these synapsin isoforms using NanoLC-ESI-MS/MS mass spectrometry. Mass spectrometry revealed that all isoforms of synapsin 1 and 2 accumulating in *Sorl1*$^{-/-}$ cortex were phosphorylated (Fig. 1B, Suppl. table 2). In most cases, synapsins were phosphorylated at site 1 (Ser9 in synapsin 1, Ser10 in synapsin 2), a site phosphorylated upon depolarization following Ca^{2+} influx. Other identified phosphorylations encompassed sites 4, 5, 6, and 7 [14]. Thus, out of eight functionally characterized phosphorylation sites in synapsins, six were present in the protein iso-spots accumulating in the SORLA-deficient cortex. Additional phosphorylations, which had been identified but not functionally characterized thus far (http://www.uniprot.org/), were also present in the accumulating synapsin 1 and 2 iso-spots (Fig. 1B, Suppl. table 2).

To substantiate the accumulation of phosphorylated (active) forms of synapsin 1 and 2 in receptor-deficient brains, we analyzed SORLA-deficient mouse cortices by 2D-

Western blotting applying antibodies that specifically recognize synapsins phosphorylated at site 1, site 4, or site 6. In line with our proteome data (Fig. 1B), synapsin 1 phosphorylated at sites 1, 4, and 6, as well as synapsin 2 phosphorylated at site 1 were significantly increased in abundance in mutant mice (Fig. 2; n=4-6, unpaired Student's *t*-test). Taken together, accumulation of multi-phosphorylated forms of synapsin 1 and 2 was identified in the *Sorl1*$^{-/-}$ brain, indicating a status of chronic activation of synapsins 1 and 2 as a consequence of SORLA deficiency.

2.3 SORLA interacts with synapsin via 14-3-3-adaptor proteins

Next to synapsins, 2D-PAGE proteome analysis also uncovered significant changes in expression levels of 14-3-3 proteins that were reduced in both cortex and hippocampus of SORLA-deficient as compared to control mice (Suppl. table 1). For cortex, the spot volume ratio *Sorl1*$^{-/-}$/*Sorl1*$^{+/+}$ for 14-3-3γ was 0.83 (p=0.024). For hippocampus, the spot volume ratios for 14-3-3α/β, 14-3-3γ, and 14-3-3ζ/δ were 0.879 (p=0.01), 0.798 (p=0.04) and 0.772 (p=0.01), respectively. 14-3-3s are abundant brain proteins that bind to motifs in target proteins characterized by phosphorylated serine or threonine residues. 14-3-3 proteins are proposed to act as scaffold enabling close proximity of heterologous proteins simultaneously bound by 14-3-3 dimers (reviewed in [15]).

Using *in silico* analysis, we identified putative 14-3-3 binding sites in synapsin 1 (Ser666), in synapsin 2 (Ser546), and in the cytoplasmic tail of SORLA (Ser2168). Phosphorylation of SORLA *in vivo* was described before [16–18]. Our phosphorylation analysis further detected phosphorylation of synapsin 1 and 2 at the putative 14-3-3 binding sites (Ser666 and Ser546) in mouse cortex, a prerequisite for 14-3-3 binding to these sites (Fig. 1B). Together, this raises the possibility of phospho-SORLA to interact with phospho-synapsins via 14-3-3 adaptors. In support of this hypothesis, the ability of SORLA, synapsin, and 14-3-3 to form a complex was confirmed by co-immunoprecipitation (coIP) of the

endogenous proteins from mouse cortical extracts using antibodies directed against SORLA (Fig. 3A, lane 4) or synapsin (Fig. 3A, lane 7). Because 14-3-3 binding sites are phospho-motifs, we also tested whether the interaction between SORLA, synapsin, and 14-3-3 was sensitive to phosphorylation. To do so, we repeated the coIP experiments using cortical lysates dephosphorylated by alkaline phosphatase treatment. The efficiency of coIP of SORLA, synapsin, and 14-3-3 from dephosphorylated cortical lysates was reduced significantly as compared to untreated samples using both anti-SORLA (Fig. 3A, lane 5) and anti-synapsin IgG (Fig. 3A, lane 8). To provide a direct proof for a 14-3-3-dependent interaction of SORLA and synapsin, we carried out coIP experiments in the presence of 14-3-3-specific antisera that block protein interactions. Under these conditions, coIP of SORLA, synapsin, and 14-3-3 was strongly impaired (Fig. 3A; lanes 6 and 9). Statistical analysis of replicate coIP experiments substantiated the significance of these findings (Fig. 3B-D, n=3-5, unpaired Student´t-test). Immunoprecipitation of SORLA and synapsin was also seen with three different 14-3-3 binding motif-specific antibodies, confirming the presence of 14-3-3 interaction sites in either of the proteins (or in both) (Fig. 3E, lanes 2-4). As these binding motif-specific antibodies only detect corresponding motifs if phosphorylated, coIP of SORLA and synapsin with these antibodies from brain documents phosphorylation of these sites in either of the proteins (or in both).

2.4 SORLA regulates synapsin expression through calpain activity

Since abundance of synapsin 1 and 2 was increased by SORLA deficiency, we wondered whether the opposite was true when the receptor was overexpressed. Thus, we analyzed lysates of the neuroblastoma cell line SH-SY5Y stably overexpressing SORLA (SY5Y-S) [5]. Synapsin levels were substantially reduced in SY5Y-S compared to parental SY5Y cells (Fig. 4A; lanes 1-4).

It has been shown before that turnover of synapsin is controlled by the calcium-activated protease calpain [19]. To evaluate whether the SORLA-dependent reduction of synapsin levels was mediated by this protease, we generated cell clones from SY5Y and SY5Y-S lines stably overexpressing a small hairpin (sh) RNA directed against calpain 1. Knock-down of calpain 1 worked equally well in both cell lines (Fig. 4B, Suppl. Fig.4A). Intriguingly, the ability of SORLA to down-regulate synapsin levels was lost when calpain 1 expression was reduced in SY5Y-S (Fig. 4A, lanes 5-8; Fig. 4C). Recruitment of calpain into a complex composed of SORLA and synapsin was substantiated by coIP experiments from mouse cortical extracts using antibodies directed against calpain 1 or calpain 2. Both primary antisera co-immunoprecipitated endogenous SORLA and synapsin, however, calpain 1 showed a stronger potential to co-immunoprecipitate SORLA as compared to calpain2 (Fig. 3E, lanes 5 and 6). So far, our studies provided evidence for the ability of SORLA to regulate the levels of expression and the phosphorylation status of synapsin 1 and 2 in cell lines and in the murine brain. The underlying mechanism possibly involves calpain-dependent turnover of this synaptic vesicle protein.

2.5 SORLA co-localizes with 14-3-3 and synapsin at synapses

Based on the ability of SORLA to co-immunoprecipitate synapsins and 14-3-3 (Fig. 3), we reasoned that SORLA, which so far was described to reside mostly in the neuronal cell soma, also localizes, at least in part, to the pre-synaptic area. Co-localization of SORLA, synapsin, and 14-3-3 in synaptic structures was substantiated by immunocytochemistry of primary mouse neurons (Fig. 5A-D) and by sub-cellular fractionation (Suppl. Fig. 3). Also, co-localization of SORLA and synapsin with calpain 1 in synaptic structures of these cells was seen (Fig. E-H). The close interaction of SORLA with synapsin, and SORLA with 14-3-3 protein in primary neurons was confirmed by proximity ligation assay, a PCR-based detection assay to demonstrate the proximity of two target proteins (Olink Bioscience;

www.olink.com). Close proximity of SORLA with 14-3-3 (Fig. 5I) or of SORLA with synapsin (Fig. 5J) was readily seen in primary mouse neurons. Lastly, close proximity of SORLA and synapsin within the range of 30 nm in primary neurons was also documented by STORM superresolution microscopy (Fig. 5K).

Collectively, our data from large-scale proteomics to cell biology studies all support a model whereby SORLA regulates the functional expression of phospho-synapsin through delivery to calpain-mediated degradation (Fig. 6).

3. DISCUSSION

Global proteome screens identified expression changes in synapsins as the most prominent and consistent feature of cortex and hippocampus proteomes in SORLA-deficient mice. Additional experimentation validated these results and revealed that phosphorylated forms of synapsin accumulated in SORLA-deficient mice (Fig. 1). Synapsins are encoded by three genes in the mammalian genome (*Synapsin I, II* and *III*) [20]. Among other functions, synapsins are proposed to tether small SV to the actin cytoskeleton, regulating the number of vesicles in nerve termini available for release [21]. Upon phosphorylation, synapsins dissociate from the cytoskeleton enabling vesicle movement [21]. In line with this model, SORLA-dependent control of phospho-synapsin levels in nerve termini may determine the distribution of SV between reserve pool and readily releasable pool, rendering this receptor a facilitator of neurotransmission and memory consolidation. This way, SORLA deficiency may contribute to synaptic dysfunction, a hallmark of AD pathology. Future studies should address this potential SORLA-dependent synaptic mechanism in more detail.

The ability of SORLA to control functional expression of synapsins is further supported by our studies in SH-SY5Y cells wherein overexpression of the receptor resulted in decreased levels of the proteins (Fig. 4). Obviously, SH-SY5Y cells lack certain features of neurons such as synapses. Thus, functional expression of synaptic vesicle proteins may not necessarily be regulated by the exact same mechanisms as in the brain (such as phosphorylation). Still, the ability of SORLA to affect synapsin expression in a calpain 1-dependent mechanism in this cell line argues for a regulatory role of this receptor in synapsin bioavailabity *in vivo*.

Our data further suggests that SORLA binds synapsins via 14-3-3 adaptor proteins, although we cannot exclude the possibility that additional proteins are involved in complex formation. 14-3-3 proteins are dimeric adaptors that bind to phospho-motifs in numerous target proteins including synapsins [22,23]. They are enriched in synaptic

compartments [24]. In chromaffin cells, blockade of 14-3-3 proteins by antibodies reduces neurotransmitter release [25,26] whereas deficiency in *Drosophila* causes impairment of synaptic transmission at the neuromuscular junction [27]. Because 14-3-3s might promote interaction of SORLA with synapsin in a phosphorylation-dependent manner, we propose the existence of a tripartite complex that regulates phosphorylation-dependent degradation of synapsins. Based on our data, complex formation identifies phospho-synapsin molecules destined for calpain-mediated degradation, a major pathway for control of synapsin turnover [19]. Importantly, shRNA-mediated knockdown of calpain in SH-SY5Y cells levitated the effect of SORLA overexpression on synapsin levels (Fig. 4).

As well as identifying a role for SORLA in control of functional expression of synapsins, our studies also suggest an intriguing link between receptor activity and neurotrophin signaling. Thus, previous data identified BDNF as a potent inducer of *Sorl1* gene transcription in neurons suggesting an interesting yet poorly understood role for SORLA as downstream effector of BDNF action regulating Aβ production as one immediate consequence [12]. In addition, it was reported that SORLA not only impacts on APP processing downstream of BDNF, but also boosts BDNF/TrkB signaling by strengthening TrkB transportation along neurites [28]. BDNF regulates synaptic plasticity [29] and acute treatment with BDNF potentiates excitatory synaptic transmission in brain slices and in neurons *in vivo* [30–32]. These short-term effects of BDNF on synaptic transmission are initiated upon binding of BDNF to its receptor TrkB, and by subsequent activation of several signaling pathways including ERK [33]. Among other downstream effects, synapsin phosphorylation is a well-documented consequence of BDNF/TrkB signaling through ERK [34]. It causes strengthening of neurotransmitter release, a short-term mode of action how BDNF participates in memory consolidation. Interestingly, more recently a study using induced pluripotent stem cells (iPSC) from patients documented, that risk haplotypes in *Sorl1* respond less to BDNF than protective haplotypes. In detail, it was reported that BDNF could

only induce *Sorl1* expression in iPSC that carried at least one protective receptor haplotype [35]. The authors also reported that, in line with previous work [36], BDNF only reduced Aβ production in cells capable of inducing SORLA, highlighting the importance of the interplay between SORLA and BDNF in the disease situation. The relevance of the here described SORLA-dependent control of synapsins should be explored in the context of BDNF-dependent synaptic modulation in AD in future studies.

4. MATERIAL AND METHODS

4.1 Materials

Antibodies directed against synapsins (Fig. 2, 3, 4; Suppl. Fig. 3); synapsin 1 (Synapsin1XP; Fig. 5), phospho-synapsin–site 1 (Fig. 2), 14-3-3γ (Fig. 3A), 14-3-3 binding motifs (Fig. 3D), calpain-1/-2 (Fig. 4, 5), and PSD-95 (Suppl. Fig. 3) were purchased from Cell Signaling Technology. Antibodies directed against synapsin 1 phosphorylated at sites 4 and 6 were purchased from Abcam (Fig. 1). Antibodies directed against synapsins phosphorylated at sites 1, 4, and 6 correspond to anti-phospho-synapsin (Ser9), anti-phospho-synapsin 1 (Ser62), and anti-phospho-synapsin 1 (Ser549), respectively, according to the originally identified phosphorylation sites in the rat [14]. Antibodies directed against 14-3-3 binding motifs correspond to motif 1 (Arg/Lys and Ser at positions -3 and -2, phospho-Ser at position 0, and Pro at position +2; "motif a", polyclonal antibody; "motif b, monoclonal antibody) and motif 2 (Phospho-(Ser) Arg-X-Tyr/Phe-X-pSer; "motif c"), respectively [37]. Additional antisera used include anti-14-3-3 pan (Fig. 3; US Biological), anti-tubulin (Calbiochem), and anti-synapsin (used for IP; SYnaptic SYstems). Rabbit N-terminal anti-SORLA serum (epitope: amino acids 54-2107 of SORLA) was produced in-house and characterized in previous studies [38,39]. The calpain 1 shRNA plasmid used for stable calpain knock-down in SH-SY5Y cells was purchased from Santa Cruz.

.

4.2 Animal and cell experimentation

The generation of *Sorl1*$^{-/-}$ mice by targeted gene disruption has been reported [5]. Animals were kept on an inbred Balb/c genetic background and compared to age- and gender-matched Balb/c wild-type controls. All animal experimentation was performed in accordance with guidelines of animal welfare after approval by local ethics committees. Primary cortical neurons were prepared from newborn Balb/c mice of either sex at postnatal day 1.

Cortices were dissociated in papain (1 hour at 37°C) and cultured on poly-D-lysine/collagen coated culture dishes. The neurons were cultured for 4-5 days in Neurobasal-A medium (Gibco) including B27 supplement (Sigma), and GlutaMAX (Invitrogen) as previously described [5].

Proteome analyses

Cortices and hippocampi were prepared from 1-month old SORLA-deficient and control male mice (n=6 per genotype). Proteins were extracted from shock-frozen tissue according to published protocols [40,41]. Protein extracts were separated using the 2D-PAGE technique as described [41]. The gel format was 40 cm (isoelectric focusing) x 30 cm (SDS-PAGE) x 0.9 mm (gel width). Two dimensional protein patterns were obtained by silver staining of gels and spot patterns were evaluated by Delta2D imaging software (version 4.0, Decodon).

For protein identification, 1.2 mg of the respective protein extracts were separated by 2D-PAGE and stained using a mass spectrometry (MS) compatible silver staining protocol [42]. Protein spots of interest were excised from 2D gels and subjected to in-gel tryptic digestion. Peptides were analyzed by an ESI-tandem -MS/MS on a LCQ Deca XP ion trap instrument with Nano-LC (Thermo Scientific). Mass spectra were analyzed using MASCOT software (version 2.2) automatically searching the SwissProt database (version 51.8, 513877 sequences). MS/MS ion search was performed with the following set of parameters: (i) taxonomy: Mus, (ii) proteolytic enzyme: trypsin, (iii) maximum of accepted missed cleavages: 1, (iv) mass value: monoisotopic, (v) peptide mass tolerance 0.8 Da, (vi) fragment mass tolerance: 0.8 Da, and (vii) variable modifications: oxidation of methionine and acrylamide adducts (propionamide) on cysteine. No fixed modifications were considered. Only proteins with scores corresponding to $p<0.05$, with at least two independent peptides identified were considered. The cut-off score for individual peptides was equivalent to $p<0.05$ for each peptide as calculated by MASCOT respectively.

With current technologies, the analysis of the whole mouse brain proteome is not possible [43]. Every available method can only detect a small part of the complex proteome present in eukaryotic tissues. A list of proteins that are covered by our methodological approach was published previously [13]. This dataset was also used as reference for enrichment analysis.

4.3 Determination of phosphorylation sites by mass spectrometry

LC-MS measurements were performed as described [44]. In brief, excised protein spots were washed with 50% (v/v) acetonitrile in 50 mM ammonium bicarbonate, shrunk by dehydration in acetonitrile, and dried in a vacuum centrifuge. The dried gel spots were incubated with either 50 ng trypsin (Promega), or 110 ng chymotrypsin (Roche Diagnostics), or 60 ng Asp-N (Roche Diagnostics) in 10 µL of 50 mM ammonium bicarbonate at 25 °C overnight. To extract the peptides, 10µL of 0.5% (v/v) trifluoroacetic acid in acetonitrile was added and the separated liquid was dried under vacuum. For MS analysis, the samples were reconstituted in 6 µL of 0.1% trifluoroacetic acid in acetonitrile/water (5:95). Peptides were analyzed by a reversed-phase capillary liquid chromatography system (Eksigent NanoLC Ultra, Axel Semrau) connected to an LTQ Orbitrap XL mass spectrometer (Thermo Scientific). LC separations were performed on a capillary column (PepMap100, C18, 3 µm, 100 Å, 250 mm × 75 µm i.d., Dionex) at an eluent flow rate of 200 nL/min using a linear gradient of 3–25% B in 75 min with further increase to 50% B at 80 min. Mobile phase A contained 0.1% formic acid in water, and mobile phase B contained 0.1% formic acid in acetonitrile. Mass spectra were acquired in a data-dependent mode with one MS survey scan (with a resolution of 60,000) in the Orbitrap and MS/MS scans of the four most intense precursor ions in the linear trap quadrupole. The processed MS/MS data and MASCOT server (version 2.2.2, Matrix Science Ltd, London) were used to search in-house against the SwissProt database (Version 2012_12, Taxonomy: mouse, 50697 sequences, 24398386 residues). The mass tolerance of precursor and sequence ions was set to 15 ppm and 0.35 Da, respectively. The search includes

variable modifications of cysteine with acrylamide, methionine oxidation, and phosphorylation of serine, threonine, or tyrosine. The maximum of 2, 5, and 2 missed cleavages was allowed for tryptic, chymotryptic, and Asp-N peptides, respectively. To identify phosphorylated synapsin peptides, probability-based scoring (MASCOT score) was used. In addition, tandem mass spectra of phosphopeptides were manually verified and compared with the theoretical fragment ions of synapsin.

4.4 Immunoprecipitation

Immunoprecipitation from mouse cortical lysates was carried out using the co-Immunoprecipitation Kit (Pierce) according to manufacturer's instructions. For antibody-based interference with co-immunoprecipitation, anti-14-3-3 pan IgG (10 ng/µl) was added to the samples and co-incubated at 37°C for 1h. Control samples without further treatment were also incubated at 37°C for 1 hour. Western blot analysis was conducted using standard protocols and blots were developed with Super Signal West Femto Chemiluminescent Substrate (Pierce). For densitometric analysis, signal intensities were quantified using Advanced Image Data Analyzer (AIDA) software (Raytest) version 3.51.)

4.5 Proximity ligation assay

Proximity ligation assay (PLA) is a PCR based detection assay to demonstrate close proximity of two target proteins (Olink Bioscience; www.olink.com). PLA was performed according to manufacturer's instruction (Duolink II Brightfield User Manual) on primary cortical neurons from wild type mice with the primary antibodies anti-SORLA, anti-Synapsin1XP (Cell Signaling), and anti-14-3-3 gamma (Cell Signaling), followed by incubation with secondary antibodies conjugated to oligonucleotides, which hybridize to subsequently added circle-forming oligonucleotides and prime a rolling circle amplification, if the antigens are located within proximity of 40 nm or less.

4.6 Stochastic Optical Reconstruction Microscopy (STORM)

For STORM superresolution microscopy primary neurons were visualized using a Nikon Eclipse Ti-E STORM microscope with Apo TIRF 100X 1.49 Oil objective, EM-CCD Camera iXon DU897 (Andor), inbuilt Perfect Focus System, and inbuilt drift control. SORLA and synapsin were stained using secondary antibodies either labeled with Atto 488 or Alexa 647 fluorophores. As buffer for imaging TRIS buffered saline (50 mM, pH=8) including 100 mM ethanolamine (MEA) and glucose oxidase (0.5 mg/ml) as well as catalase (40 µg/ml) together with 10% glucose was used.

Statistical analyses

For proteomic analyses datasets were analyzed using a paired two-tailed Student's t-test as SORLA-deficient and control samples were always handled in pairs starting with protein extraction until after completion of 2-D gel runs. Only spot volume ratios ≥ 20% were considered (n = 6 biological replicates, significance threshold $p \leq 0.05$). Normality of data was evaluated using Kolmogorov-Smirnov testing [40].

Enrichment analysis based on gene ontology terms was conducted by applying the following settings provided by WebGestalt: Hypergeometric test; $p \leq 0.05$; more than 2 proteins per category. The set of proteins altered by SORLA deficiency was compared to the mouse genome dataset provided by WebGestalt or to a dataset of proteins present on 2-D gels of brain tissue as reference, respectively [13].

For densitometric quantifications of Western blots, statistical tests applied and numbers of biological replicates (n) are given in the respective figure legends. Box plots depict medians as well as lower quartile, upper quartile, and sample maxima.

Acknowledgements:

We thank TE. Willnow for providing resources and for his input on the manuscript. We are indebted to M. Schmeisser, B. Tachu, Z. Cseresnyes, Y. Kläre, and A. Krajewski for expert technical support. Studies were funded in part by grants from the American Health Assistance Foundation (to MR) and the Deutsche Forschungsgemeinschaft (to DH). The authors declare no conflicts of interest.

REFERENCES

[1] Jacobsen L, Madsen P, Moestrup SK, Lund AH, Tommerup N, Nykjaer A, et al. Molecular characterization of a novel human hybrid-type receptor that binds the alpha2-macroglobulin receptor-associated protein. J Biol Chem 1996;271:31379–83. doi:10.1074/jbc.271.49.31379.

[2] Dodson SE, Andersen OM, Karmali V, Fritz JJ, Cheng D, Peng J, et al. Loss of LR11/SORLA enhances early pathology in a mouse model of amyloidosis: evidence for a proximal role in Alzheimer's disease. J Neurosci 2008;28:12877–86. doi:10.1523/JNEUROSCI.4582-08.2008.

[3] Marcusson EG, Horazdovsky BF, Cereghino JL, Gharakhanian E, Emr SD. The sorting receptor for yeast vacuolar carboxypeptidase Y is encoded by the VPS10 gene. Cell 1994;77:579–86. doi:10.1016/0092-8674(94)90219-4.

[4] Hu F, Padukkavidana T, Vægter CB, Brady OA, Zheng Y, Mackenzie IR, et al. Sortilin-mediated endocytosis determines levels of the frontotemporal dementia protein, progranulin. Neuron 2010;68:654–67. doi:10.1016/j.neuron.2010.09.034.

[5] Andersen OM, Reiche J, Schmidt V, Gotthardt M, Spoelgen R, Behlke J, et al. Neuronal sorting protein-related receptor sorLA/LR11 regulates processing of the amyloid precursor protein. Proc Natl Acad Sci U S A 2005;102:13461–6. doi:10.1073/pnas.0503689102.

[6] Rogaeva E, Meng Y, Lee JH, Gu Y, Kawarai T, Zou F, et al. The neuronal sortilin-related receptor SORL1 is genetically associated with Alzheimer disease. Nat Genet 2007;39:168–77. doi:10.1038/ng1943.

[7] Baum AE, Akula N, Cabanero M, Cardona I, Corona W, Klemens B, et al. A genome-wide association study implicates diacylglycerol kinase eta (DGKH) and several other genes in the etiology of bipolar disorder. Mol Psychiatry 2008;13:197–207. doi:10.1038/sj.mp.4002012.

[8] Offe K, Dodson SE, Shoemaker JT, Fritz JJ, Gearing M, Levey AI, et al. The lipoprotein receptor LR11 regulates amyloid beta production and amyloid precursor protein traffic in endosomal compartments. J Neurosci 2006;26:1596–603. doi:10.1523/JNEUROSCI.4946-05.2006.

[9] Schmidt V, Sporbert A, Rohe M, Reimer T, Rehm A, Andersen OM, et al. SorLA/LR11 regulates processing of amyloid precursor protein via interaction with adaptors GGA and PACS-1. J Biol Chem 2007;282:32956–64. doi:10.1074/jbc.M705073200.

[10] Rohe M, Carlo AS, Breyhan H, Sporbert A, Militz D, Schmidt V, et al. Sortilin-related receptor with A-type repeats (SORLA) affects the amyloid precursor protein-dependent stimulation of ERK signaling and adult neurogenesis. J Biol Chem 2008;283:14826–34. doi:10.1074/jbc.M710574200.

[11] Willnow TE, Carlo A-S, Rohe M, Schmidt V. SORLA/SORL1, a neuronal sorting receptor implicated in Alzheimer's disease. Rev Neurosci 2010;21:315–29. doi:10.1515/REVNEURO.2010.21.4.315.

[12] Rohe M, Synowitz M, Glass R, Paul SM, Nykjaer A, Willnow TE. Brain-derived neurotrophic factor reduces amyloidogenic processing through control of SORLA gene expression. J Neurosci 2009;29:15472–8. doi:10.1523/JNEUROSCI.3960-09.2009.

[13] Rohe M, Nebrich G, Klein O, Mao L, Zabel C, Klose J, et al. Kainate promotes alterations in neuronal RNA splicing machinery. J Proteome Res 2011;10:1459–67. doi:10.1021/pr101008p.

[14] Cesca F, Baldelli P, Valtorta F, Benfenati F. The synapsins: Key actors of synapse function and plasticity. Prog Neurobiol 2010;91:313–48. doi:10.1016/j.pneurobio.2010.04.006.

[15] Mackintosh C. Dynamic interactions between 14-3-3 proteins and phosphoproteins regulate diverse cellular processes. Biochem J 2004;381:329–42. doi:10.1042/BJ20031332.

[16] Willnow TE, Andersen OM. Sorting receptor SORLA – a trafficking path to avoid Alzheimer disease. J Cell Sci 2013;126:2751–60. doi:10.1242/jcs.125393.

[17] Lane RF, Gatson JW, Small S a, Ehrlich ME, Gandy S. Protein kinase C and rho activated coiled coil protein kinase 2 (ROCK2) modulate Alzheimer's APP metabolism and phosphorylation of the Vps10-domain protein, SorL1. Mol Neurodegener 2010;5:62. doi:10.1186/1750-1326-5-62.

[18] Herskowitz JH, Seyfried NT, Gearing M, Kahn R a, Peng J, Levey AI, et al. Rho kinase II phosphorylation of the lipoprotein receptor LR11/SORLA alters amyloid-beta production. J Biol Chem 2011;286:6117–27. doi:10.1074/jbc.M110.167239.

[19] Murrey HE, Gama CI, Kalovidouris SA, Luo W-I, Driggers EM, Porton B, et al. Protein fucosylation regulates synapsin Ia/Ib expression and neuronal morphology in primary hippocampal neurons. Proc Natl Acad Sci U S A 2006;103:21–6. doi:10.1073/pnas.0503381102.

[20] Kao HT, Porton B, Czernik AJ, Feng J, Yiu G, Häring M, et al. A third member of the synapsin gene family. Proc Natl Acad Sci U S A 1998;95:4667–72.

doi:10.1073/pnas.95.8.4667.

[21] Shupliakov O, Haucke V, Pechstein A. How synapsin I may cluster synaptic vesicles. Semin Cell Dev Biol 2011;22:393–9. doi:10.1016/j.semcdb.2011.07.006.

[22] Angrand P-O, Segura I, Völkel P, Ghidelli S, Terry R, Brajenovic M, et al. Transgenic mouse proteomics identifies new 14-3-3-associated proteins involved in cytoskeletal rearrangements and cell signaling. Mol Cell Proteomics 2006;5:2211–27. doi:10.1074/mcp.M600147-MCP200.

[23] Hosaka M, Südhof TC. Homo- and heterodimerization of synapsins. J Biol Chem 1999;274:16747–53. doi:10.1074/jbc.274.24.16747.

[24] Martin H, Rostas J, Patel Y, Aitken A. Subcellular localisation of 14-3-3 isoforms in rat brain using specific antibodies. J Neurochem 1994;63:2259–65. doi:10.1046/j.1471-4159.1994.63062259.x.

[25] Chamberlain LH, Roth D, Morgan A, Burgoyne RD. Distinct effects of ??-SNAP, 14-3-3 proteins, and calmodulin on priming and triggering of regulated exocytosis. J Cell Biol 1995;130:1063–70. doi:10.1083/jcb.130.5.1063.

[26] Wu YN, Vu ND, Wagner PD. Anti-(14-3-3 protein) antibody inhibits stimulation of noradrenaline (norepinephrine) secretion by chromaffin-cell cytosolic proteins. Biochem J 1992;285 (Pt 3:697–700.

[27] Broadie K, Rushton E, Skoulakis EMC, Davis RL. Leonardo, a drosophila 14-3-3 protein involved in learning, regulates presynaptic function. Neuron 1997;19:391–402. doi:10.1016/S0896-6273(00)80948-4.

[28] Rohe M, Hartl D, Fjorback AN, Klose J, Willnow TE. SORLA-mediated trafficking of TrkB enhances the response of neurons to BDNF. PLoS One 2013;8:e72164. doi:10.1371/journal.pone.0072164.

[29] Lewin GR, Barde YA. Physiology of the neurotrophins. Annu Rev Neurosci 1996;19:289–317. doi:10.1146/annurev.neuro.19.1.289.

[30] Figurov A, Pozzo-Miller LD, Olafsson P, Wang T, Lu B. Regulation of synaptic responses to high-frequency stimulation and LTP by neurotrophins in the hippocampus. Nature 1996;381:706–9. doi:10.1038/381706a0.

[31] Levine ES, Dreyfus CF, Black IB, Plummer MR. Brain-derived neurotrophic factor rapidly enhances synaptic transmission in hippocampal neurons via postsynaptic tyrosine kinase receptors. Proc Natl Acad Sci U S A 1995;92:8074–7.

doi:10.1073/pnas.92.17.8074.

[32] Lohof AM, Ip NY, Poo MM. Potentiation of developing neuromuscular synapses by the neurotrophins NT-3 and BDNF. Nature 1993;363:350–3. doi:10.1038/363350a0.

[33] Reichardt LF. Neurotrophin-regulated signalling pathways. Philos Trans R Soc Lond B Biol Sci 2006;361:1545–64. doi:10.1098/rstb.2006.1894.

[34] Jovanovic JN, Czernik AJ, Fienberg AA, Greengard P, Sihra TS. Synapsins as mediators of BDNF-enhanced neurotransmitter release. Nat Neurosci 2000;3:323–9. doi:10.1038/73888.

[35] Young J, Boulanger-Weill J, Williams D, Woodruff G, Buen F, Herrera C, et al. Elucidating molecular phenotypes caused by the SORL1 Alzheimer's disease genetic risk factor using human induced pluripotent stem cells. Cell Stem Cell 2015;Apr2:373–85.

[36] Carlo A-S, Gustafsen C, Mastrobuoni G, Nielsen MS, Burgert T, Hartl D, et al. The pro-neurotrophin receptor sortilin is a major neuronal apolipoprotein E receptor for catabolism of amyloid-β peptide in the brain. J Neurosci 2013;33:358–70. doi:10.1523/JNEUROSCI.2425-12.2013.

[37] Yaffe MB, Rittinger K, Volinia S, Caron PR, Aitken A, Leffers H, et al. The Structural Basis for 14-3-3:Phosphopeptide Binding Specificity. Cell 1997;91:961–71. doi:10.1016/S0092-8674(00)80487-0.

[38] Gliemann J, Hermey G, Nykjaer A, Petersen CM, Jacobsen C, Andreasen P a. The mosaic receptor sorLA/LR11 binds components of the plasminogen-activating system and platelet-derived growth factor-BB similarly to LRP1 (low-density lipoprotein receptor-related protein), but mediates slow internalization of bound ligand. Biochem J 2004;381:203–12. doi:10.1042/BJ20040149.

[39] Andersen OM, Schmidt V, Spoelgen R, Gliemann J, Behlke J, Galatis D, et al. Molecular Dissection of the Interaction between Amyloid Precursor Protein and Its Neuronal Trafficking Receptor SorLA / LR11 †. Biochemistry 2006;85:2618–28. doi:10.1021/bi052120v.

[40] Hartl D, Rohe M, Mao L, Staufenbiel M, Zabel C, Klose J. Impairment of adolescent hippocampal plasticity in a mouse model for Alzheimer's disease precedes disease phenotype. PLoS One 2008;3.

[41] Zabel C, Mao L, Woodman B, Rohe M, Wacker MA, Kläre Y, et al. A large number of protein expression changes occur early in life and precede phenotype onset in a mouse model for huntington disease. Mol Cell Proteomics 2009;8:720–34.

doi:10.1074/mcp.M800277-MCP200.

[42] Nebrich G, Herrmann M, Sagi D, Klose J, Giavalisco P. High MS-compatibility of silver nitrate-stained protein spots from 2-DE gels using ZipPlates and AnchorChips for successful protein identification. Electrophoresis 2007;28:1607–14. doi:10.1002/elps.200600656.

[43] Ahrens CH, Brunner E, Qeli E, Basler K, Aebersold R. Generating and navigating proteome maps using mass spectrometry. Nat Rev Mol Cell Biol 2010;11:789–801. doi:10.1038/nrm2973.

[44] Lange S, Sylvester M, Schümann M, Freund C, Krause E. Identification of phosphorylation-dependent interaction partners of the adapter protein ADAP using quantitative mass spectrometry: SILAC vs 18O-labeling. J Proteome Res 2010;9:4113–22. doi:10.1021/pr1003054.

FIGURES

A

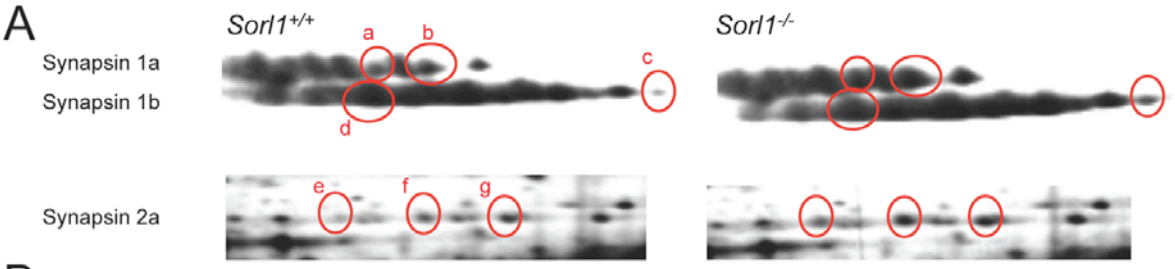

B

Spot ID	Gene Name	p-value	Ratio (*Sorl1*$^{-/-}$ / *Sorl1*$^{+/+}$)	Protein Name	Identified Phosphorylations
a	Syn1	0.038	1.526	Synapsin-1a	Ser 9/11 (1), Ser 62/67 (4,5), Ser 553/551 (7,6), Ser 568 (2), Ser 510/ Tyr 512, Ser 642, Ser 427, Ser 664/666, Ser 682/684
b	Syn1	0.035	1.608	Synapsin-1a	Ser 9/11 (1), Ser 62/67 (4,5), Ser 553/551 (7,6), Ser 682/684, Ser 510/ Tyr 512, Ser 642, Ser 427, Ser 664/666
c	Syn1	0.015	1.339	Synapsin-1b	Ser 9/11 (1)
d	Syn1	0.009	1.235	Synapsin-1b	Ser 9/11 (1), Ser 62/67 (4,5), Ser 553/551 (7,6), Ser 568 (2), Ser 510/ Tyr 512, Ser 642, Ser 427, Ser 664/666
e	Syn2	0.047	1.451	Synapsin-2a	Ser 426, Ser 546/544
f	Syn2	0.005	1.706	Synapsin-2a	Ser 10 (1), Ser 426, Ser 546/544
g	Syn2	0.035	1.815	Synapsin-2a	Ser 10 (1)

Figure 1. SORLA deficiency results in accumulation of synapsin 1 and 2 in the cortex.

(A) Segments of large two-dimensional polyacrylamide gels of cortical proteins from *Sorl1*$^{+/+}$ and *Sorl1*$^{-/-}$ mice stained with silver nitrate are shown. An exemplary complete gel is shown in Suppl. Fig. 1. Red circles highlight protein spots corresponding to isoforms of synapsin 1a, 1b, and 2a that are significantly altered in SORLA-deficient as compared to wild type cortices (Spot ID a - g). **(B)** List of protein iso-spots of synapsin 1a, 1b, and 2a that are significantly altered in the cortex of *Sorl1*$^{-/-}$ compared to control mice (n=6 per genotype; paired two-tailed Student's *t*-test, $p<0.05$). The phosphorylation sites identified for the respective iso-spots by NanoLC-ESI-MS/MS mass spectrometry are also given. Numbers in brackets refer to the numbering of synapsin phosphorylation sites 1 through 8 as described in [14]. A slash between two modification sites indicates that an unambiguous assignment of phosphorylation site was not possible.

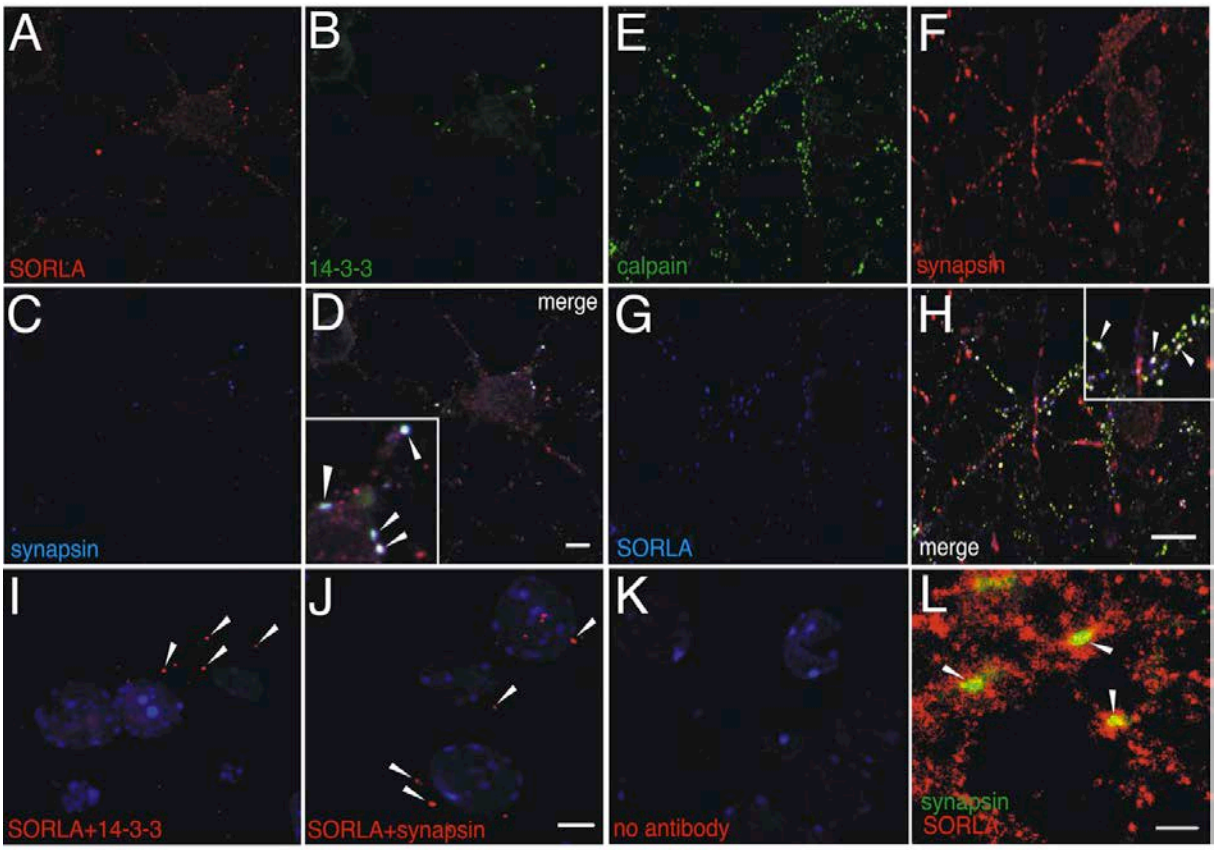

Figure 2. Increased phosphorylation of isoforms of synapsin 1 and 2 in *Sorl1*$^{-/-}$ mice.

(A) Small two-dimensional polyacrylamide gels of cortical proteins from *Sorl1*$^{+/+}$ and *Sorl1*$^{-/-}$ cortices were subjected to Western blot analysis using antibodies specific for phospho-synapsins 1 and 2 isoforms phosphorylated at p-site 1, p-site 4, or p-site 6. **(B)** Densitometric quantifications of Western blots as exemplified in (A) document significant accumulation of synapsin 1 phosphorylated at site 1, site 4, and site 6, as well as synapsin 2a phosphorylated at site 1 in *Sorl1*$^{-/-}$ cortex as compared to controls (n=4-6, unpaired Student's t-test).

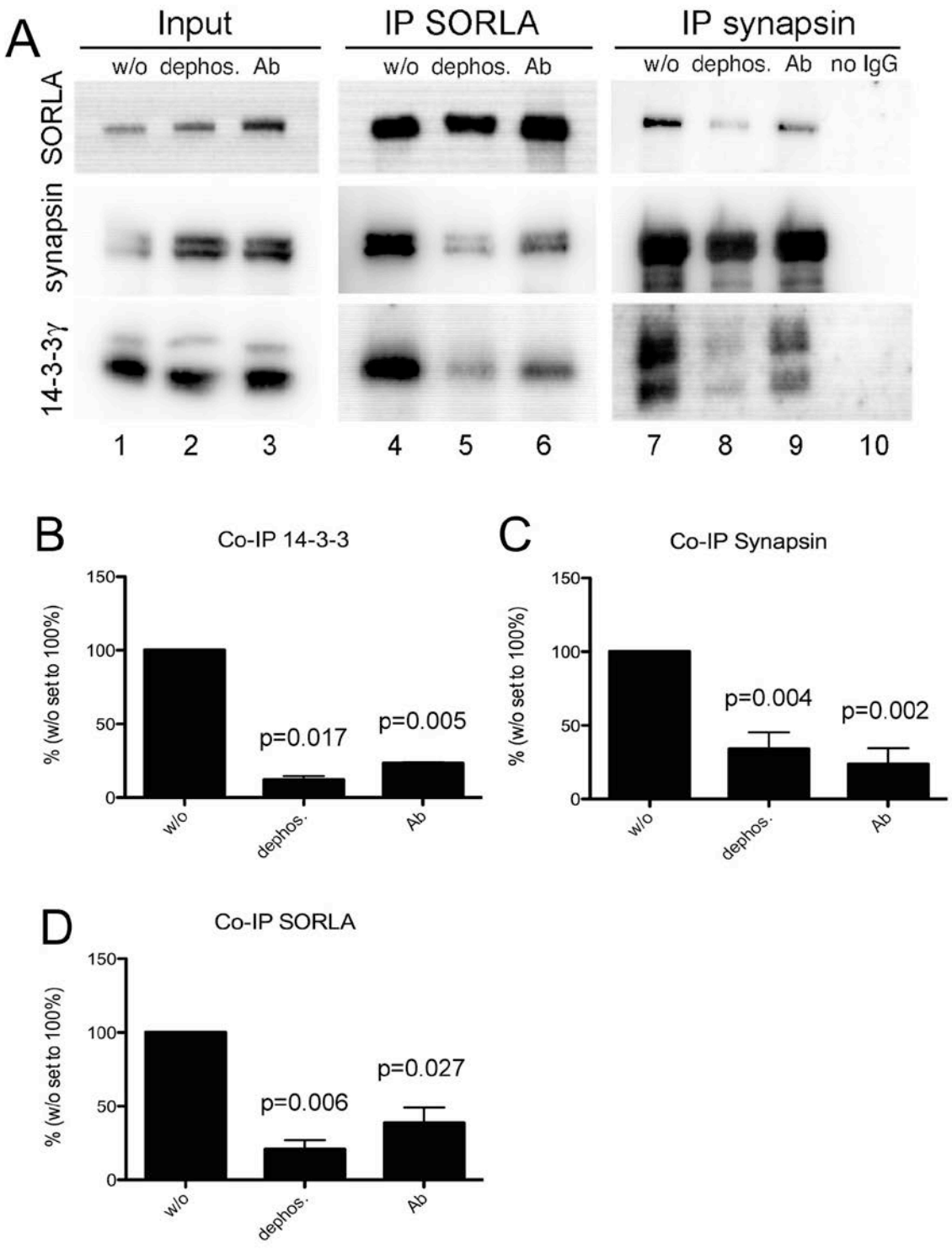

Figure 3. Phosphorylation-dependent interaction of SORLA with synapsin and 14-3-3.

(A) Immunoprecipitation of SORLA (IP SORLA; lanes 4 - 6) or synapsin (IP synapsin; lanes 7 - 10) from total mouse cortical lysates either untreated (w/o), treated with alkaline phosphatase (dephos.), or incubated with pan-14-3-3 antibodies (Ab). Co-

immunoprecipitation of the indicated proteins was confirmed by Western blot analyses. Efficient co-immunoprecipitation of SORLA, synapsin, and 14-3-3 is seen in untreated tissues (lanes 4 and 7), but to a lesser extent from dephosphorylated (lanes 5 and 8) or from anti-14-3-3 IgG treated samples (lanes 6 and 9). Lanes 1 - 3 depict the presence of SORLA, synapsin, and 14-3-3 in cortical lysates prior to immunoprecipitation. Lane 10 indicates lack of co-immunoprecipitation of SORLA, synapsin, and 14-3-3 in the absence of primary antibody. **(B - D)** Quantification of co-immunoprecipitation results as exemplified in panel A by densitometric scanning of Western blots documents significantly impaired coIP of 14-3-3 (B), synapsin (C), and SORLA (D) in dephosphorylated (dephos.) or 14-3-3 antibody-treated (Ab.) conditions as compared to untreated controls (w/o; set to 100%) (n=3-5, unpaired Student's t-test). (**E**) Co-immunoprecipitation of SORLA and synapsin from total mouse cortical lysates using three different antibodies directed against 14-3-3 binding motifs (lanes 2 - 4) or antisera directed against calpain 1 (lane 5) or calpain 2 (lane 6). No co-immunoprecipitation was observed in conditions lacking primary antibody (lane 7). The presence of SORLA and synapsin in the brain lysate prior to immunoprecipitation is shown in lane 1 (Input).

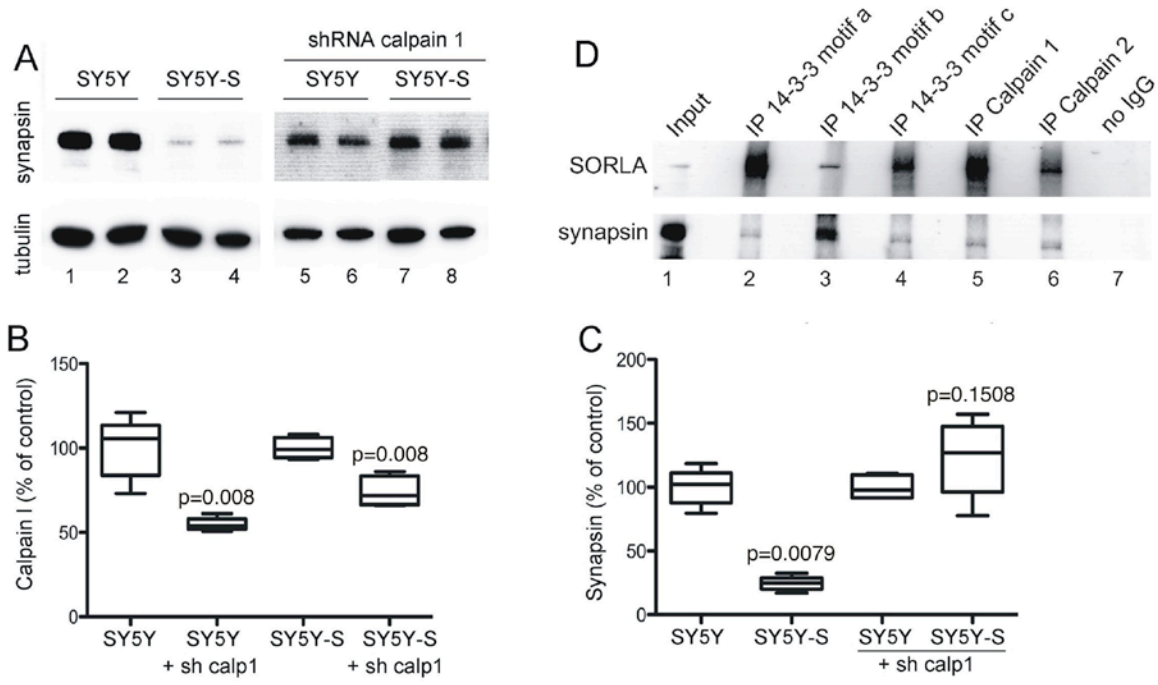

Figure 4. SORLA modulates calpain-dependent turnover of synapsin.

(A) Western blot analysis demonstrates reduced levels of synapsins in SH-SY5Y cells overexpressing SORLA (SY5Y-S; lanes 3 - 4) compared to the parental cell line (SY5Y; lanes 1 - 2). No difference in synapsin levels between the two cell lines is seen when expression of calpain 1 is blocked by a small hairpin (sh) RNA (lanes 5 – 8). Detection of tubulin served as loading control. **(B)** Loss of calpain 1 expression works equally well in SY5Y and SY5Y-S cells expressing a shRNA directed against calpain 1 (+ shCalp1) compared to the untreated cell lines (mean set at 100%) as determined by replicate Western blot analyses (n=5; p=0.008, Mann-Whitney-U). **(C)** Quantification of synapsin levels in the indicated cell lines by densitometric scanning of replicate Western blots. Synapsin levels are significantly reduced in untreated SY5Y-S compared with parental cells (mean set at 100%) (n=5; p=0.0079, Mann-Whitney-U). In contrast, no difference in synapsin levels is seen when cells lack calpain 1 expression (n=5; p=0.1508, Mann-Whitney-U).

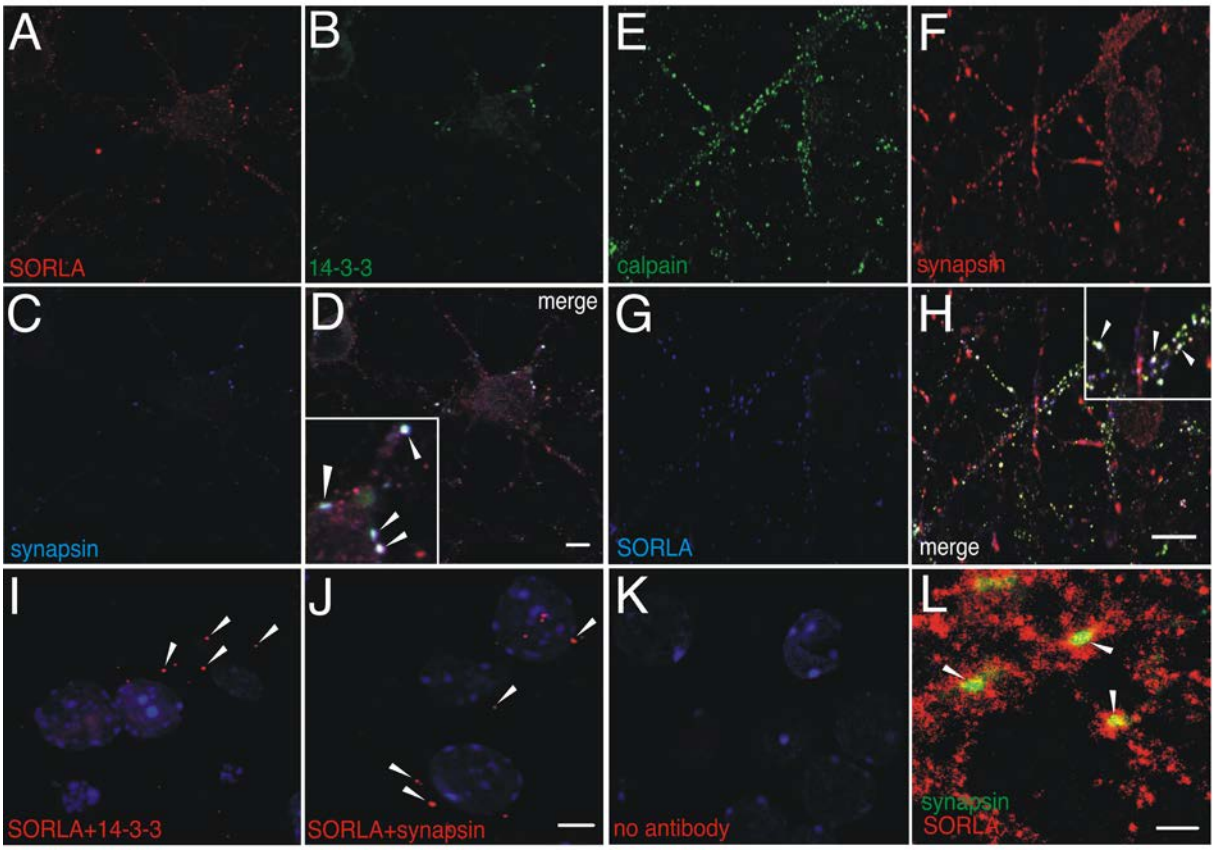

Rohe et al., Figure 5

Figure 5. SORLA colocalizes with synapsin and 14-3-3 at synapses.

(A-D) Immunocytochemical detection of SORLA (red), synapsin (blue), and 14-3-3 (green) in primary mouse neurons using confocal microscopy. Co-localization in synaptic structures is indicated in the inset to the merged micrograph by arrowheads. Scale bar: 20 µm. (**E-H**) Immunocytochemical detection of SORLA (blue), synapsin (red), and calpain (green) in primary mouse neurons using confocal microscopy. Co-localization of all three proteins in synaptic structures is indicated in the inset to the merged micrograph by arrowheads. Scale bar: 20 µm. (**I-K**) Proximity ligation assays (PLA) for SORLA and 14-3-3 (I) and for SORLA and synapsin (J) are shown. Red dots indicted close proximity of the respective proteins (arrowheads). No PLA signal is when omitting the primary antibodies as negative control (K). Close proximity of the respective proteins is indicated by red signals. Nuclei are stained with DAPI. Scale bar: 5µm. **(L)** STORM superresolution microscopy for SORLA (red) and

synapsin (green) in primary neurons. Arrowheads highlight close interaction of the proteins in synaptic structures. Scale bar: 700 nm.

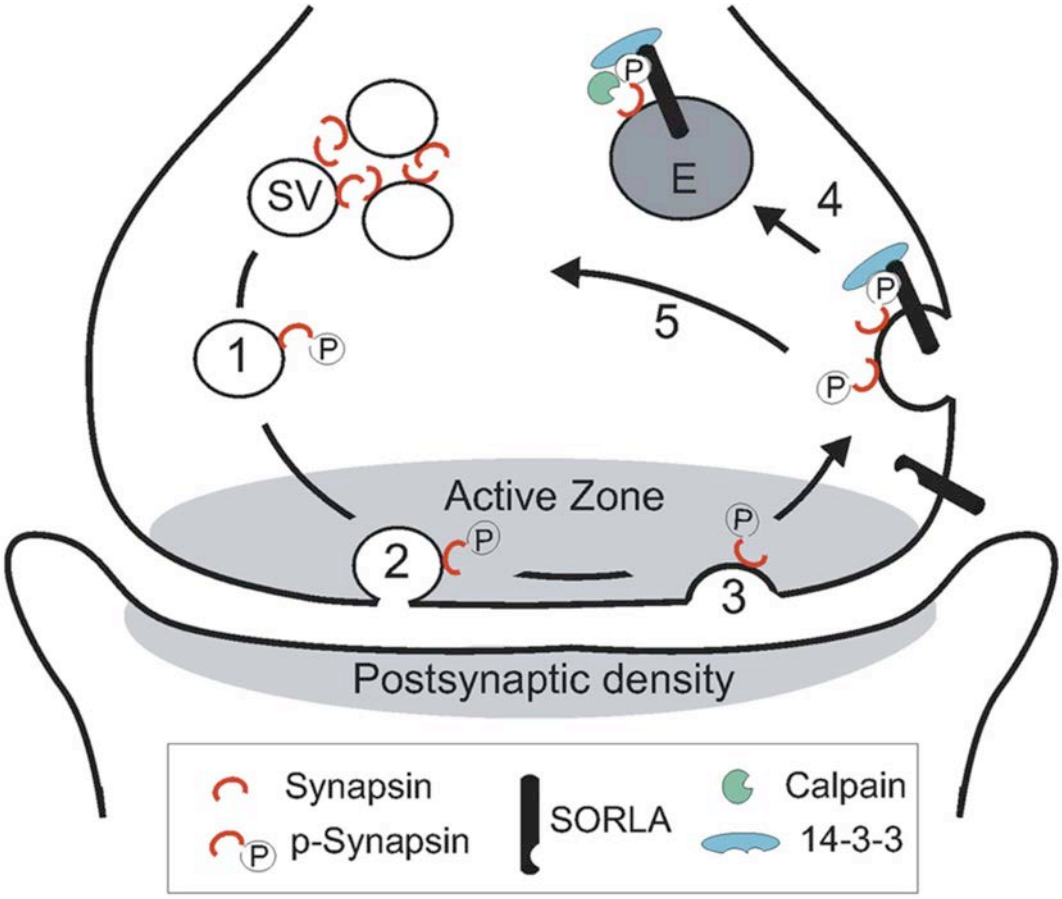

Figure 6. Proposed function of SORLA in control of synapsin activity.

Unphosphorylated synapsin promotes clustering of synaptic vesicles (SV) in the reserve pool of the nerve terminus. Upon phosphorylation of synapsin, SV dissociate from this cluster and enter the active zone to dock with the presynaptic plasma membrane (step 1). A fusion pore opens and neurotransmitters are released into the synaptic cleft (step 2). In the peri-active zone, inward budding of the plasma membrane forms new SV that carry p-synapsin (step 3). Phosphorylated forms of SORLA and p-synapsin complex via 14-3-3 adapter proteins delivering p-synapsin to calpain-dependent degradation associated with synaptic endosomes

(step 4). SV not tagged by SORLA are recycled back to the SV cluster (step 5). According to this model, loss of SORLA activity results in an increased fraction of vesicles carrying p-synapsin molecules, thereby causing an overall larger pool of mobilized SV.